Published in final edited form as:
Nat Genet. ; 44(4): 420–S2. doi:10.1038/ng.2204.

Common genetic variants at the 11q13.3 renal cancer susceptibility locus influence binding of HIF to an enhancer of cyclin D1 expression

Johannes Schödel[1,*], **Chiara Bardella**[2], **Lina K Sciesielski**[1], **Jill M Brown**[3], **Chris W Pugh**[1], **Veronica Buckle**[3], **Ian P Tomlinson**[2,4], **Peter J Ratcliffe**[1,*], and **David R Mole**[1,*]

[1]Henry Wellcome Building for Molecular Physiology, University of Oxford, Oxford, OX3 7BN, United Kingdom

[2]Molecular and Population Genetics Laboratory, The Wellcome Trust Centre for Human Genetics, University of Oxford, Oxford, OX3 7BN, United Kingdom

[3]Weatherall Institute of Molecular Medicine, John Radcliffe Hospital, University of Oxford, Oxford OX4 9DS, United Kingdom

[4]Oxford NIHR Comprehensive Biomedical Research Centre, The Wellcome Trust Centre for Human Genetics, University of Oxford, Oxford, OX3 7BN, United Kingdom

Abstract

Though genome-wide association studies (GWAS) have identified the existence of numerous population-based cancer susceptibility loci, mechanistic insights remain limited, particularly for intergenic polymorphisms. Here we show that polymorphism at a remote intergenic region on chromosome 11q13.3, recently identified as a susceptibility locus for renal cell carcinoma[1], modulates the binding and function of hypoxia inducible factor (HIF) at a previously unrecognized, transcriptional enhancer of cyclin D1 specific for renal cancers characterized by pVHL inactivation. The protective haplotype impairs binding of HIF-2 resulting in an allelic imbalance in cyclin D1 expression, thus affecting a link between hypoxia pathways and cell cycle control.

Kidney cancer accounts for more than 100,000 deaths per year world-wide[2]. More than 80% are clear cell tumors (ccRCCs) and the majority are associated with loss of function of the von Hippel Lindau (pVHL) tumor suppressor[3,4]. pVHL is an ubiquitin ligase that promotes oxygen-dependent degradation of hypoxia-inducible transcription factors (HIF-1α and HIF-2α), by recognizing hydroxylated prolyl residues in HIF-α[5-7]. Loss of pVHL function up-regulates HIF-α subunits, and activates HIF-dependent transcriptional pathways. Given the common occurrence, but uncertain or poorly understood causality, of dysregulated hypoxia pathways in cancer, this has raised fundamental questions as to whether and by what means the HIF pathway contributes to ccRCC. Though a range of other (non-HIF)

*To whom correspondence may be addressed: Peter J Ratcliffe (pjr@well.ox.ac.uk), David R Mole (drmole@well.ox.ac.uk) or Johannes Schödel (schoedel@well.ox.ac.uk), Henry Wellcome Building for Molecular Physiology, University of Oxford, Oxford, OX3 7BN, United Kingdom. Tel: 44(0)1865 287788; Fax: 44(0)1865 287787. .

Author Contributions JS, CWP, VB, IT, PJR, DRM designed research. JS, CB, LKS, JB, VB, DRM performed experiments. JS, CB, LKS, JB, VB, IT, PJR, DRM analyzed data. JS, PJR, DRM wrote the manuscript.

Datasets and Accession Numbers The data discussed in this publication have been deposited in NCBI's Gene Expression Omnibus (Schödel et al., 2012) and are accessible through GEO Series accession number GSE34871 (http://www.ncbi.nlm.nih.gov/geo/query/acc.cgi?acc=GSE34871).

Competing financial interests No competing financial interests to declare.

Europe PMC Funders Author Manuscripts

functions have been identified for pVHL[8], which may contribute to tumor suppressor behavior, gene transfer and knock-down studies point to a role for HIF-2, but not HIF-1, in progression of ccRCC xenografts[8-13]. However, so far, there has been little evidence from human genetics of a direct causal role for HIF in sporadic ccRCC. Genetic analyses of RCC tumor material have not identified activating mutations in *EPAS1* (encoding HIF-2α and, surprisingly, the only genetic alterations in genes encoding HIF sub-units have been inactivating mutations or deletions of *HIF1A* (encoding HIF-1α)[13-16].

However, a recent GWAS discovered two SNPs in intron 1 of *EPAS1* that were significantly associated with increased RCC risk, though no functional studies were performed[1]. In the same study, a second RCC-susceptibility locus was identified in an intergenic region of unknown function on 11q13.3, a finding that has recently been replicated in other populations[17,18]. As part of an ongoing study to define the direct transcriptional targets of HIF-2 in renal cancer, we undertook a genome-wide analysis of HIF-2-binding sites in pVHL-defective 786-O cells (that lack functional HIF-1α due to a truncated transcript[13]) using chromatin immunoprecipitation with antibodies directed against HIF-2α and its dimerization partner HIF-1β coupled to high-throughput sequencing (ChIP-seq).

Amongst approximately 600 pangenomic HIF-2 ChIP signals, we observed strong binding (ranked 12th by peak height) almost precisely coinciding with the RCC predisposition SNP rs7105934 on 11q13.3. The strongest signal (H) was observed 5 kb centromeric to rs7105934 (chr11: 68,943,716 - 68,944,005). More minor signals were observed immediately adjacent (h1) and more distally (h2) (Fig. 1a). None of these regions bound HIF subunits in a previous ChIP-seq analysis in pVHL-competent MCF-7 breast cancer cells[19]. Analysis of data from Europeans in the 1000 Genomes project (http://www.1000genomes.org/) showed that the major ChIP-seq signal (H) overlapped polymorphic nucleotides: rs7948643, rs7939721 and rs7939830 whereas rs17136556, rs77247065 and rs11263441 overlapped the weaker signal (h2). Pairwise linkage disequilibrium (LD) of all these SNPs and the RCC-associated SNP, rs7105934, was reported to be very high ($r^2 = 1$, from 1000 Genomes Pilot 1 data). To confirm this directly, we genotyped a larger cohort of 192 cancer-free individuals from the UK at each SNP and confirmed strong LD (r^2 ranging from 0.77 to 1), especially between rs7105934 and SNPs overlying the strongest HIF-2 ChIP signal (Fig. 1a). Sequence inspection indicated that sites (H) and (h2), but not (h1) contained consensus HRE motifs (RCGTG, Supplemental Fig. 1). ChIP-qPCR confirmed robust binding of HIF-2α and HIF-1β at the major site (H) in both 786-0 and human RCC tissue, whereas signals at (h2) were much less robust, particularly for HIF-2α (Fig. 1b, c and data not shown). Thus LD at the intergenic 11q13.3 RCC risk-associated locus extends across a region (H) of robust HIF-2-binding in RCC.

Since this locus is remote from the nearest annotated gene, and lacks CpG islands associated with gene promoters, we determined whether the major HRE-containing site (H) had the epigenetic characteristics of a transcriptional enhancer. First, we examined for reduced nucleosome occupancy using formaldehyde-assisted isolation of regulatory elements (FAIRE)[20]. This revealed a region of reduced nucleosome occupancy extending over approximately 2 kb around the HIF-binding site in 786-0, but not MCF-7 cells, (Fig.2a). Second, in 786-0 but not MCF7 cells we observed high levels of H3K4me1 and H3K27ac, with low levels of H3K4me3, a combination of histone modifications observed at active enhancers (compare *NDRG1* enhancer) but not promoters (compare *FAM13A* promoter) (Fig. 2b-d)[21-23]. As expected for an active enhancer, in 786-0 cells low-level ChIP-qPCR signal for RNApol2 was also observed, consistent with interaction with the transcriptional apparatus (Fig. 2e)[21]. Finally, in 786-O cells expression of the reporter gene was enhanced by these sequences and attenuated by mutation of the HRE (Fig. 2f). Taken together, these

data indicate that the 11q13.3 RCC susceptibility locus overlaps a HIF-dependent transcriptional enhancer.

Genome-wide expression analysis in 786-O cells and renal tumors identified *CCND1* flanking the site and lying 220 kb telomeric to the enhancer as one of the most HIF-regulated genes on chromosome 11 (Supplemental Fig. 2a, b). *CCND1* is an oncogene that is commonly up-regulated in cancer including RCC[24-26] (Supplemental Fig. 2c). Previous studies have defined *CCND1* as a HIF-regulated gene in 786-0 and other RCC cell lines but were unable to map the control sequences[10,27-30]. These analyses revealed striking cell-type specificity; *CCND1* being responsive to HIF-2α in RCC cells but not in any other cell analyzed. We therefore tested whether this tight cell-type specificity was reflected in the HIF-2-binding and epigenetic enhancer marks at the 11q13.3 susceptibility locus. Both DNA accessibility, as determined by FAIRE, and HIF-2-binding, assessed by ChIP-qPCR, were similarly cell-type specific, being present in all pVHL-defective RCC cell lines tested but absent across cell lines expressing wild-type pVHL (including cancerous (Caki-1) and non cancerous (HK-2, HKC-8) renal epithelial cells), (Fig. 3a, b) despite comparable levels of HIF-2α induced by hydroxylase inhibition (Supplemental Fig. 3a). Similar cell-type specific patterns of HIF-1 binding were observed; HIF-1-binding in all pVHL-defective RCC cell lines that express this isoform, but absent in all cell lines expressing wild-type pVHL (Supplemental Fig. 3c). Furthermore, consistent with previously reported patterns of cyclin D1 expression in RCC cell lines, the 11q13.3 enhancer remained accessible and able to bind HIF following re-introduction of wild type pVHL into pVHL-defective RCC cells (786-0/VHL cells)[19,27](Fig. 3c, d). Thus constitutively high levels of HIF are not required to maintain the activity of this region as an enhancer, but it is a stable feature of cell lines derived from pVHL-defective RCC.

Exact concordance between the existence of the HIF-binding enhancer and the regulation of cyclin D1 by HIF strongly suggested that the 11q13.3 locus encodes a long-range enhancer that physically associates with the *CCDN1* promoter to regulate transcription. To test this, we used two assays of physical association between distant genetic loci; high-resolution fluorescent *in situ* hybridization (FISH) and chromatin conformation capture (3C)[31]. Both techniques provided evidence for physical association of the HIF-binding enhancer with the *CCDN1* promoter in 786-O cells, but not MCF-7 cells (Fig. 4 and Supplemental Fig. 4). Although our analysis does not exclude the possibility that the enhancer regulates additional genes we conclude that the 11q13.3 susceptibility locus overlaps a cell-type specific, long-range enhancer of cyclin D1 expression.

We next examined the effect of variants at 11q13.3 on the enhancer and on expression of cyclin D1. We first genotyped a number of pVHL-defective ccRCC cell lines at rs7105934, rs7948643 and rs77247065 and found one, KTCL140, to be heterozygous at all three SNPs (and at the remaining 4 SNPs covered by the other ChIP-seq peaks) with normal copy number and equal allelic dosage (Supplemental Fig. 5). Allele-specific analysis of immunoprecipitated chromatin in this cell line demonstrated preferential binding of both HIF-2α and HIF-1β to the major (RCC-predisposing) allele at rs7948643 (Fig. 5a). ChIP using an antibody directed against RNApol2 also showed that the major allele at this locus preferentially interacted with the basal transcriptional machinery (Fig. 5b). Furthermore, similar analysis of material prepared from KTCL140 cells by FAIRE indicated a greater degree of chromatin accessibility in the major allele at this locus (Fig. 5c). Thus the minor (RCC-protective) allele at 11q13.3 disrupts HIF-binding, DNA accessibility and interaction with the transcriptional apparatus at the *CCND1* enhancer.

We then determined whether these allele-specific effects at the *CCND1* enhancer alter the allelic balance of cyclin D1 expression. We identified heterozygous SNPs (rs7177 and

rs678653) within the 3′ UTR of *CCND1* in KTCL140 cells. These SNPs are in weak LD with SNPs at the HIF-binding site (for the tagSNP rs7105934, pairwise LD with rs7177 is r^2=0.02, D'=0.51 and with rs678653 is r^2=0.00, D'=0.08). The phase in KTCL140 cells is therefore unknown. However, mRNA from these cells showed distinct ($p<10^{-3}$) allelic imbalance compared to genomic DNA (Fig. 5d and Supplemental Fig. 6a). Furthermore, similar allelic imbalance was seen in RNApol2 binding to this coding region (Fig. 5e and Supplemental Fig. 6b). These results are therefore consistent with the prediction of differential cyclin D1 expression arising from the two 11q13.3 alleles in these cells.

Taken together, these findings indicate that the activity of a promoter-distant enhancer of cyclin D1 that binds HIF-2 in renal cancer is reduced by the protective haplotype at the 11q13.3 renal cancer susceptibility locus. Given the established role of cyclin D1 as an oncogenic cell cycle regulator[26] this provides a plausible mechanism for the observed susceptibility effects. High LD in this region makes it difficult to distinguish the causative polymorphism(s) genetically. Although two of the SNPs in the susceptibility haplotype (rs7948643 and rs7939721) lie only 10bp and 15bp from the HIF-binding motif at 11q13.3 (H), neither disrupts the core RCGTG sequence. Thus, whether the minor allele affects HIF-binding directly or indirectly by altering local chromatin structure remains to be determined. Interestingly, although, as with most HIF binding sites, the enhancer can bind both HIF-1 and HIF-2, functional studies of cyclin D1 expression suggest that only HIF-2 is transcriptionally active[10], a result which is in keeping with transcriptional selectivity among HIF isoforms being conferred by post-DNA-binding mechanisms[32,33].

Although, we have not tested every wild-type pVHL cell, the enhancer activity appears to be restricted to p*VHL*-defective RCC cells, but is not reversed by re-introduction of pVHL suggesting that it is a specific feature of the pVHL-defective RCC background. This raises interesting questions as to when, during RCC development, the susceptibility effect operates and whether it contributes to the tissue-specificity of pVHL tumor suppressor behavior. Kidneys of patients with *VHL* disease (the principal familial form of RCC) contain large numbers of tiny 'precursor lesions' representing foci of biallelic *VHL* inactivation[34]. These manifest up-regulation of the HIF pathway. However, only a minority expresses HIF-2α and cyclin D1; this pattern being strongly associated with dysplastic morphology[10]. This suggests that, at least in this form of RCC, either the HIF-2-*CCDN1* link results from a 'second hit' occurring after biallelic *VHL* inactivation (perhaps due to epigenetic alterations creating a 'neo-enhancer'[15,16,35,36]) or that the unusual connection between the HIF pathway and *CCND1* is an intrinsic property of a rare population of cells in the renal tubular epithelium that are then selected following dysregulation of the *VHL*-HIF pathway. A third possibility is that stable epigenetic changes are effected as a result of long-term HIF activation following pVHL inactivation and that these are not reversible upon re-expression of wild-type pVHL.

The finding that both major RCC-predisposition loci defined by GWAS, 2p21 (*EPAS1* encoding HIF-2α) and 11q13.3 affect specific components of hypoxia pathways suggests that particular aspects of hypoxia pathway dysregulation (as opposed to general up-regulation) are important in RCC development. A third locus at 12q24.31 (within intron 1 of *SCARB1*) that was implicated in the original GWAS, but not robustly in the replication cohorts[1], lies within 2 kb of an additional HIF-binding site identified in multiple cell-types (Supplemental Fig. 7). However, LD with the candidate SNP at 12q24.31 did not extend over this HIF-binding region, indicating that if this is an RCC-predisposition locus then it is unlikely to operate through direct effects on HIF-binding *per se*. Nevertheless, consideration of other GWAS signals in the light of our pan-genomic analysis of HIF-binding in RCC, (http://www.ncbi.nlm.nih.gov/) may yield further insights into the role of hypoxia pathways in RCC predisposition.

Methods

Cell culture - 786-O and MCF-7 cells were purchased from ATCC. HKC-8 cells were provided by L. Racusen, 786-O cells re-expressing pVHL were a gift from W. G. Kaelin Jr. RCC4 cells were a gift from C.H. Buys, and all other RCC cells were from M. Lerman. All cell lines were grown in Dulbecco's modified Eagle's Medium, 100U/ml penicillin, 100μg/ml streptomycin and 10% fetal bovine serum (Sigma). HKC-8 cells were cultured in Dulbecco's modified Eagle's medium/Ham's F-12 supplemented with 10% fetal calf serum, 2mM L-glutamine, 100U/ml penicillin and 100 μg/ml streptomycin, 5 μg/ml insulin, 5 μg/ml transferring, and 5ng/ml selenium (Sigma). As indicated sub confluent cell cultures were exposed to 1mM dimethyloxalyl glycine (DMOG, Frontier Scientific) or 1% O2 for 16h prior to harvest.

Tumor samples - were provided by A. L. Harris and collected in accordance with the World Medical Association Declaration of Helsinki.

Chromatin immunoprecipitation

The chromatin immunoprecipitations (ChIP) were performed on cell lines as previously described[19,38], using antibodies against HIF-1α (PM14), HIF-2α (PM9), HIF-1β (Novus Biologicals, NB100-110), RNA polymerase II (Santa Cruz SC-899), H3K4me1 (Abcam ab8895), H3K4me3 (Cell signaling 9751), H3K27ac (Abcam ab4729). Pre-immune serum or IgG (Millipore 12-370) were used as negative controls as applicable. For ChIP from tumors snap-frozen tissue was pulverized, resuspended in PBS and fixed with 1% formaldehyde for 12 minutes at 4°C. Cross linking was quenched by addition of 125 mM glycine. After washing in PBS the tissue was lysed in SDS buffer for 15 minutes at room temperature and sheared using an Ultra-Turrax®. Sonication was carried out as described[19] and for each IP the volume of chromatin corresponding to 25 mg of initial tissue weight was used.

High throughput sequencing

Library preparations and sequencing was carried out as described[19]. Sequences were mapped to NCBI build 36 (hg18) and two-sample peak finding was undertaken using the CisGenome software suite (http://www.biostat.jhsph.edu/~hji/cisgenome/).

RNA isolation and expression arrays

RNA was isolated using Tri Reagent (Sigma) and transcribed into cDNA using the high capacity cDNA reverse transcription kit (Applied Biosystems, Life Technologies, Carlsbad, California). Microarray analysis of 786-O cells treated with control siRNA or siRNA targeting HIF-2α or of 786-O/VHL cells exposed to normoxia and hypoxia (1% O_2) for 16h were carried out in triplicates using Illumina WG6 Bead Chip at the Microarray facility of the Wellcome Trust Centre for Human Genetics, Oxford, UK, and values were normalized and filtered for present/absent calls using the Affymetrix software.

Immunoblotting

Cells were lysed in UREA/SDS buffer and proteins were resolved by SDS-PAGE. After transferring the proteins onto PVDF membranes HIF proteins were detected using mouse monoclonal anti-HIF-1α (BD Bioscience 610958) and anti-HIF-2α (190b) antibodies and horseradish peroxidase-conjugated anti-mouse secondary antibodies (Dako).

Formaldehyde - assisted isolation of regulatory elements (FAIRE)

Following protocols from Giresi et al.[20] an aliquot from cross linked and sonicated ChIP chromatin was used. DNA was extracted with phenol chloroform, precipitated and purified using a PCR product 'clean up' kit (Sigma). qPCR was performed on FAIRE DNA and input DNA in which cross-linking was reversed prior to phenol chloroform extraction. Values were normalized to input DNA and compared to a region just outside of the putative regulatory region (for 11q13.3, hg18 chr11:68948541-68948669; for *NDRG1*, hg18 chr8:134458206-134458299). Primer sequences are available upon request.

Transfection assays

Transfections of plasmids and a β-galactosidase reporter were performed in 786-O cells using Fugene® 6 reagents (Promega). Cells were harvested after 48h and luciferase activity in extracts was measured using a Luciferase reporter assay system (Promega). Values were normalized to β-galactosidase activity. Sequences were ligated into the Bgl2 restriction site of the pGL3 promoter vector (Promega) using PCR amplified genomic DNA from 786-O cells spanning 227bp (hg18 Chr11: 68943675-68943901) of the major peak (H) or 1453bp (hg18 Chr11: 68943675-68945127) including both the major (H) and minor (h1) peaks. Mutations of HREs (RCGTG into RCATA) were performed using site directed mutagenesis. All constructs were sequence verified. Primer sequences are available upon request.

DNA fluorescence in situ hybridization

Fosmids spanning the region of interest were labeled by nick translation with biotin or digoxigenin as previously described[39] (*CCND1* gene: G248P85537B2, hg18 chr11: 69147108-69190642, HIF-binding site: G248P83053H10, hg18 chr11: 68921622-68961904, 227kb centromeric of HIF-binding site: G248P85591A1, hg18 chr11: 68697196-68733066, 227kb telomeric of gene: G248P89319G2, hg18 chr11: 69380087-69418798). 2D FISH was performed as described previously[40] except that slides were denatured at 72°C and probes were denatured at 85°C for 10 min. For each probe pair, inter-probe distances were measured in micrometers using ImageJ software[41] in approximately 100 nuclei. 3D FISH was also performed as previously described[40] except that cells were permeabilised in 0.5% Triton X-100 in PBS followed by quenching in 0.276% ammonium chloride in PBS for 10 min at RT. Cells were denatured in a 1 in 4.5 dilution of conc. HCl in milliQ water. Slides were hybridized overnight at 37 °C. Images were captured on a Zeiss 510 confocal microscope. Z stacks were taken of each nucleus at 400nm steps. For each probe pair, inter-probe distances were measured in micrometers using Zeiss LSM software and nuclear volume measurements in ImageJ software using the Voxel Counter plug-in in approximately 100 nuclei. Non-parametric statistical analysis was by Kruskal-Wallis 1-way ANOVA and by Mann-Whitney U-test (SPSS 19).

Chromatin conformation capture assay

Experiments were performed according to protocols in Hagege et al.[42] with some modifications. Cells were grown in 15cm dishes with (MCF-7) or without (786-O) 1mM DMOG for 4h. Cells were cross-linked using 1.5 mM Di(N-succinimidyl) glutarate (Sigma) for 45 min at room temperature followed by 1% formaldehyde (Sigma) for 10min and quenching by 0.125 M glycine (Sigma). After cell lysis, EcoR1 (New England Biolabs) digest was carried out at 37°C overnight. Fragments were diluted 1:8 in ligation buffer and ligation was carried out for 4 h at 16° C. Cross-linking was reversed at 65°C overnight and DNA was isolated using phenol chloroform extraction. Digest efficiency was monitored using primers spanning restriction sites and by comparison of digested to non-digested DNA. Chromatin interaction was interrogated using quantitative PCR employing a forward primer and a fluorescence labeled probe located at the first *ECOR1* restriction site

downstream of the HIF-binding locus (anchor site) combined with reverse primers covering *ECOR1* restriction sites across the region of interest. Two BAC clones (RP11 266K14 and RP11 378K8) covering the region of interest were used to create an artificial library of ligation products in order to normalize for PCR efficiency. Data were normalized to the signal from the BAC clone library and, between cell lines, by reference to a region at the *EEF1G* locus[43]. Primer sequences are available upon request.

DNA extraction - DNA was extracted from blood samples using DNeasy® Blood and Tissue from QuiagenR (Alameda, CA), following the manufacturer's instructions. The DNA samples were quantified using PicoGreen® (Invitrogen).

Allele specific assays - Linkage disequilibrium of SNPs in vicinity of the HIF-binding peaks (rs4980785, rs7948643, rs7939721, rs7939830, rs17136556, rs77247065, rs11263441 with the tag SNP rs7105934 on 11q13.3 and rs4765621 with the tagSNP rs4765623 on 12q24.31) was verified in a cohort of 192 cancer-free control individuals using competitive allele-specific PCR KASPar chemistry (KBiosciences Ltd, Hertfordshire, UK). Haploview software (www.broadinstitute.org) was used to define the haplotype blocks and recombination hotspots. To identify samples heterozygous for the common and rare alleles at rs7105934, rs7948643 and rs77247065, pVHL-defective ccRCC cell lines were genotyped using KASPar. For the heterozygous (1:1 allelic dosage) cell line KTCL140, genomic DNA derived from ChIP or FAIRE (two to three independent biological samples) or cDNA generated from DNAse-treated mRNA were genotyped at rs7948643 and the *CCND1* 3′UTR SNPs rs7177 and rs678653, using allele-specific Taqman® assay (Applied Biosystems). Constitutional DNA from individuals known to be homozygous or heterozygous at each SNP was included in each assay as a reference. All primers, probes and conditions used are available on request. We additionally analyzed allele-specific expression at rs7177 using the method of Lo et al[44] which uses one allele as test and the other as reference in a manner analogous to conventional RT-qPCR for mRNA expression levels based on a standard curve. This provided confirmatory evidence of the shift in allelic dosage found by Taqman®-based SNP analysis (data not shown). The KTCL140 cell line DNA was also genotyped using the Illumina OmniExpress SNP array according to the manufacturer's protocols. The data analysis was performed using Illumina Genomestudio software.

Data analysis

Statistical analyses for FISH measurements were as stated and performed using IBM SPSS Statistics version 19 (SPSS Inc). Statistical analyses for FAIRE and ChIP results were performed using a one-sample t-test comparing the mean with a hypothetical value of 1 using GraphPadPrism Version 4.00 (GraphPad Software Inc). All other analyses were conducted using a one-way anova with Dunnett's post-test.

Supplementary Material

Refer to Web version on PubMed Central for supplementary material.

Acknowledgments

This work was funded by the Wellcome Trust (088182/Z/09/Z to JS, 078333/Z/05/Z, WT091857MA), the Higher Education Funding Council for England, the German Research Foundation (SC 132/2-1 to LKS), and by Urology Cancer Research and Education UCARE (Oxford). Samples of renal tumors were a kind gift from A. L. Harris through the Oxford Radcliffe Biobank - Oxford Biomedical Research Centre. HKC-8 cells were provided by L. Racusen, 786-O cells re-expressing pVHL were a gift from W. G. Kaelin Jr. RCC4 cells were a gift from C.H. Buys, and all other RCC cells were from M. Lerman.

References

1. Purdue MP, et al. Genome-wide association study of renal cell carcinoma identifies two susceptibility loci on 2p21 and 11q13.3. Nat Genet. 2011; 43:60–5. [PubMed: 21131975]
2. Ferlay J, et al. Estimates of worldwide burden of cancer in 2008: GLOBOCAN 2008. Int J Cancer. 2010; 127:2893–917. [PubMed: 21351269]
3. Gnarra JR, et al. Mutations of the VHL tumour suppressor gene in renal carcinoma. Nat Genet. 1994; 7:85–90. [PubMed: 7915601]
4. Herman JG, et al. Silencing of the VHL tumor-suppressor gene by DNA methylation in renal carcinoma. Proc Natl Acad Sci U S A. 1994; 91:9700–4. [PubMed: 7937876]
5. Maxwell PH, et al. The tumour suppressor protein VHL targets hypoxia-inducible factors for oxygen-dependent proteolysis. Nature. 1999; 399:271–5. [PubMed: 10353251]
6. Jaakkola P, et al. Targeting of HIF-alpha to the von Hippel-Lindau ubiquitylation complex by O2-regulated prolyl hydroxylation. Science. 2001; 292:468–72. [PubMed: 11292861]
7. Ivan M, et al. HIFalpha targeted for VHL-mediated destruction by proline hydroxylation: implications for O2 sensing. Science. 2001; 292:464–8. [PubMed: 11292862]
8. Kaelin WG Jr. The von Hippel-Lindau tumour suppressor protein: O2 sensing and cancer. Nat Rev Cancer. 2008; 8:865–73. [PubMed: 18923434]
9. Kondo K, Kim WY, Lechpammer M, Kaelin WG Jr. Inhibition of HIF2alpha is sufficient to suppress pVHL-defective tumor growth. PLoS Biol. 2003; 1:E83. [PubMed: 14691554]
10. Raval RR, et al. Contrasting properties of hypoxia-inducible factor 1 (HIF-1) and HIF-2 in von Hippel-Lindau-associated renal cell carcinoma. Mol Cell Biol. 2005; 25:5675–86. [PubMed: 15964822]
11. Yan Q, Bartz S, Mao M, Li L, Kaelin WG Jr. The hypoxia-inducible factor 2alpha N-terminal and C-terminal transactivation domains cooperate to promote renal tumorigenesis in vivo. Mol Cell Biol. 2007; 27:2092–102. [PubMed: 17220275]
12. Gordan JD, et al. HIF-alpha effects on c-Myc distinguish two subtypes of sporadic VHL-deficient clear cell renal carcinoma. Cancer Cell. 2008; 14:435–46. [PubMed: 19061835]
13. Shen C, et al. Genetic and Functional Studies Implicate HIF1alpha as a 14q Kidney Cancer Suppressor Gene. Cancer Discov. 2011; 1:222–235. [PubMed: 22037472]
14. Morris MR, et al. Mutation analysis of hypoxia-inducible factors HIF1A and HIF2A in renal cell carcinoma. Anticancer Res. 2009; 29:4337–43. [PubMed: 20032376]
15. Dalgliesh GL, et al. Systematic sequencing of renal carcinoma reveals inactivation of histone modifying genes. Nature. 2010; 463:360–3. [PubMed: 20054297]
16. Varela I, et al. Exome sequencing identifies frequent mutation of the SWI/SNF complex gene PBRM1 in renal carcinoma. Nature. 2011; 469:539–42. [PubMed: 21248752]
17. Wu X, et al. A genome-wide association study identifies a novel susceptibility locus for renal cell carcinoma on 12p11.23. Hum Mol Genet. 2011 [PubMed: 22010048]
18. Cao Q, et al. Chromosome 11q13.3 variant modifies renal cell cancer risk in a Chinese population. Mutagenesis. 2011 [PubMed: 22131124]
19. Schodel J, et al. High-resolution genome-wide mapping of HIF-binding sites by ChIP-seq. Blood. 2011; 117:e207–17. [PubMed: 21447827]
20. Giresi PG, Kim J, McDaniell RM, Iyer VR, Lieb JD. FAIRE (Formaldehyde-Assisted Isolation of Regulatory Elements) isolates active regulatory elements from human chromatin. Genome Res. 2007; 17:877–85. [PubMed: 17179217]
21. Heintzman ND, et al. Distinct and predictive chromatin signatures of transcriptional promoters and enhancers in the human genome. Nat Genet. 2007; 39:311–8. [PubMed: 17277777]
22. Creyghton MP, et al. Histone H3K27ac separates active from poised enhancers and predicts developmental state. Proc Natl Acad Sci U S A. 2010; 107:21931–6. [PubMed: 21106759]
23. Rada-Iglesias A, et al. A unique chromatin signature uncovers early developmental enhancers in humans. Nature. 2011; 470:279–83. [PubMed: 21160473]
24. Gumz ML, et al. Secreted frizzled-related protein 1 loss contributes to tumor phenotype of clear cell renal cell carcinoma. Clin Cancer Res. 2007; 13:4740–9. [PubMed: 17699851]

25. Kaelin WG Jr. Treatment of kidney cancer: insights provided by the VHL tumor-suppressor protein. Cancer. 2009; 115:2262–72. [PubMed: 19402056]
26. Musgrove EA, Caldon CE, Barraclough J, Stone A, Sutherland RL. Cyclin D as a therapeutic target in cancer. Nat Rev Cancer. 2011; 11:558–72. [PubMed: 21734724]
27. Zatyka M, et al. Identification of cyclin D1 and other novel targets for the von Hippel-Lindau tumor suppressor gene by expression array analysis and investigation of cyclin D1 genotype as a modifier in von Hippel-Lindau disease. Cancer Res. 2002; 62:3803–11. [PubMed: 12097293]
28. Bindra RS, Vasselli JR, Stearman R, Linehan WM, Klausner RD. VHL-mediated hypoxia regulation of cyclin D1 in renal carcinoma cells. Cancer Res. 2002; 62:3014–9. [PubMed: 12036906]
29. Baba M, et al. Loss of von Hippel-Lindau protein causes cell density dependent deregulation of CyclinD1 expression through hypoxia-inducible factor. Oncogene. 2003; 22:2728–38. [PubMed: 12743597]
30. Wykoff CC, et al. Gene array of VHL mutation and hypoxia shows novel hypoxia-induced genes and that cyclin D1 is a VHL target gene. Br J Cancer. 2004; 90:1235–43. [PubMed: 15026807]
31. Dekker J, Rippe K, Dekker M, Kleckner N. Capturing chromosome conformation. Science. 2002; 295:1306–11. [PubMed: 11847345]
32. Hu CJ, Sataur A, Wang L, Chen H, Simon MC. The N-terminal transactivation domain confers target gene specificity of hypoxia-inducible factors HIF-1alpha and HIF-2alpha. Mol Biol Cell. 2007; 18:4528–42. [PubMed: 17804822]
33. Lau KW, Tian YM, Raval RR, Ratcliffe PJ, Pugh CW. Target gene selectivity of hypoxia-inducible factor-alpha in renal cancer cells is conveyed by post-DNA-binding mechanisms. Br J Cancer. 2007; 96:1284–92. [PubMed: 17387348]
34. Mandriota SJ, et al. HIF activation identifies early lesions in VHL kidneys: evidence for site-specific tumor suppressor function in the nephron. Cancer Cell. 2002; 1:459–68. [PubMed: 12124175]
35. Xia X, et al. Integrative analysis of HIF binding and transactivation reveals its role in maintaining histone methylation homeostasis. Proc Natl Acad Sci U S A. 2009; 106:4260–5. [PubMed: 19255431]
36. Krieg AJ, et al. Regulation of the histone demethylase JMJD1A by hypoxia-inducible factor 1 alpha enhances hypoxic gene expression and tumor growth. Mol Cell Biol. 2010; 30:344–53. [PubMed: 19858293]
37. Pescador N, et al. Identification of a functional hypoxia-responsive element that regulates the expression of the egl nine homologue 3 (egln3/phd3) gene. Biochem J. 2005; 390:189–97. [PubMed: 15823097]

References for Methods section

38. Mole DR, et al. Genome-wide association of hypoxia-inducible factor (HIF)-1alpha and HIF-2alpha DNA binding with expression profiling of hypoxia-inducible transcripts. J Biol Chem. 2009; 284:16767–75. [PubMed: 19386601]
39. Brown J, et al. Subtelomeric chromosome rearrangements are detected using an innovative 12-color FISH assay (M-TEL). Nat Med. 2001; 7:497–501. [PubMed: 11283680]
40. Brown JM, et al. Coregulated human globin genes are frequently in spatial proximity when active. J Cell Biol. 2006; 172:177–87. [PubMed: 16418531]
41. Abramoff MD, Magalhaes PJ, Ram SJ. Image Processing with ImageJ. Biophotonics International. 2004; 11:36–42.
42. Hagege H, et al. Quantitative analysis of chromosome conformation capture assays (3C-qPCR). Nat Protoc. 2007; 2:1722–33. [PubMed: 17641637]
43. Ramachandrareddy H, et al. BCL6 promoter interacts with far upstream sequences with greatly enhanced activating histone modifications in germinal center B cells. Proc Natl Acad Sci U S A. 2010; 107:11930–5. [PubMed: 20547840]
44. Lo HS, et al. Allelic variation in gene expression is common in the human genome. Genome Res. 2003; 13:1855–62. [PubMed: 12902379]

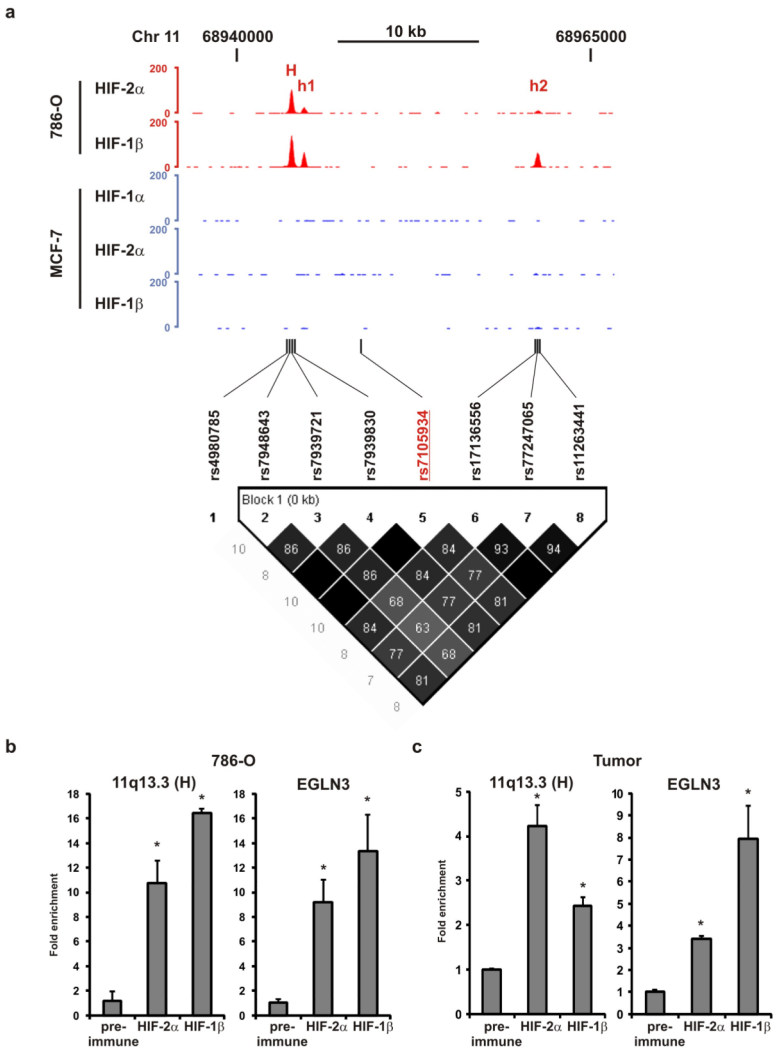

Figure 1. HIF-binding at 11q13.3

(a) Genome Browser tracks showing the read density at the 11q13.3 locus for HIF-2α and HIF-1β ChIP-seq in 786-O cells and for HIF-1α, HIF-2α and HIF-1β ChIP-seq in MCF-7 cells in which HIF-α chains were stabilized by hydroxylase inhibition. Three HIF-2-binding sites (H, h1 and h2) are identified in 786-O but not MCF-7 cells. Also shown are the positions of genotyped SNPs, together with LD analysis (r^2 values). SNPs overlapping peak H and peak h2 are in sufficiently strong LD with the disease-associated tagSNP, rs7105934 (red) that the latter can act as a simple proxy. **(b, c)** ChIP-qPCR analysis confirming HIF-2α and HIF-1β binding at 11q13.3 (H) in both 786-0 cells **(b)** and renal tumor tissue **(c);** for comparison ChIP-qPCR at an established HIF-binding site at the *EGLN3* locus[33,37] is shown. Bars show mean ± SD (n=3); *p<0.05, compared to pre-immune serum.

Europe PMC Funders Author Manuscripts

Europe PMC Funders Author Manuscripts

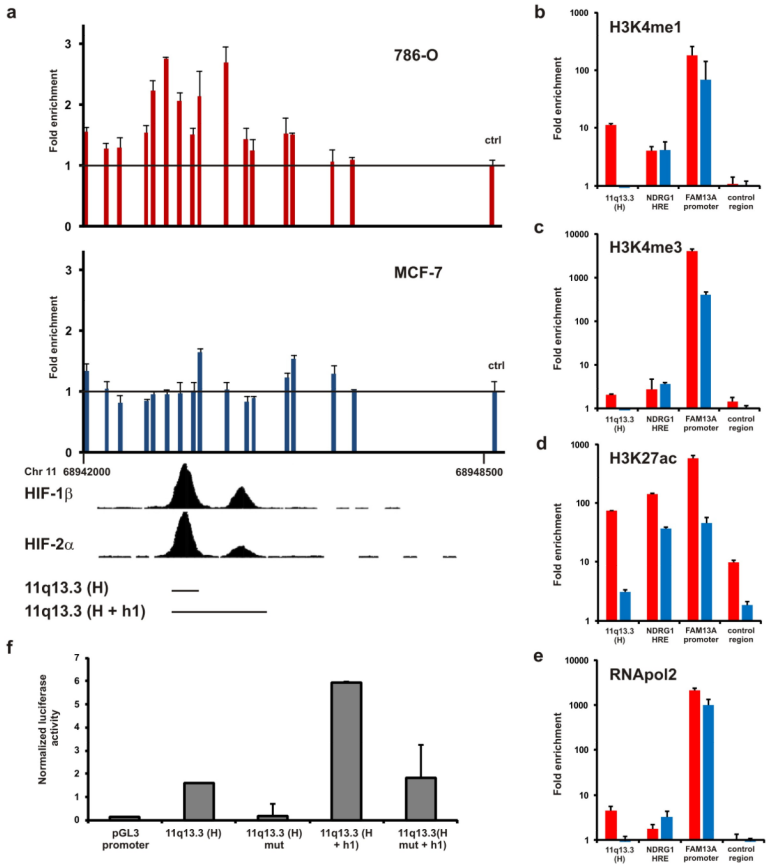

Figure 2. Chromatin structure and function of an enhancer at 11q13.3

(a) Formaldehyde-assisted isolation of regulatory elements (FAIRE) was performed in 786-O and MCF-7 cells to map nucleosome occupancy at the 11q13.3 locus. qPCR products were normalized to those obtained for input DNA at this locus and then related to values obtained at a nearby control region outside the putative enhancer (ctrl, far right bar). Data is plotted against chromosomal location; the position of the ChIP-seq signals for HIF-1β and HIF-2α is illustrated below. **(b-e)** ChIP-qPCR signals at 11q13.3 (H) obtained from 786-0 cells (red) or MCF-7 cells (blue) using antibodies against **(b)** H3K4me1, **(c)** H3K4me3, **(d)** H3K27ac and **(e)** RNApol2; for comparison signals at a ubiquitous HIF-binding enhancer (*NDRG1,* Supplemental Fig. 3b), a HIF-binding promoter (*FAM13A1)* and a nearby non-enhancer control region are shown. **(f)** Luciferase reporter assay performed in 786-O cells using the sequences 11q13.3 (H) or 11q13.3 (H+h1) (indicated above); mut indicated mutation of the core HRE motif in H. Data is normalized to co-transfected β-galactosidase activity, mean ± SD (n=3).

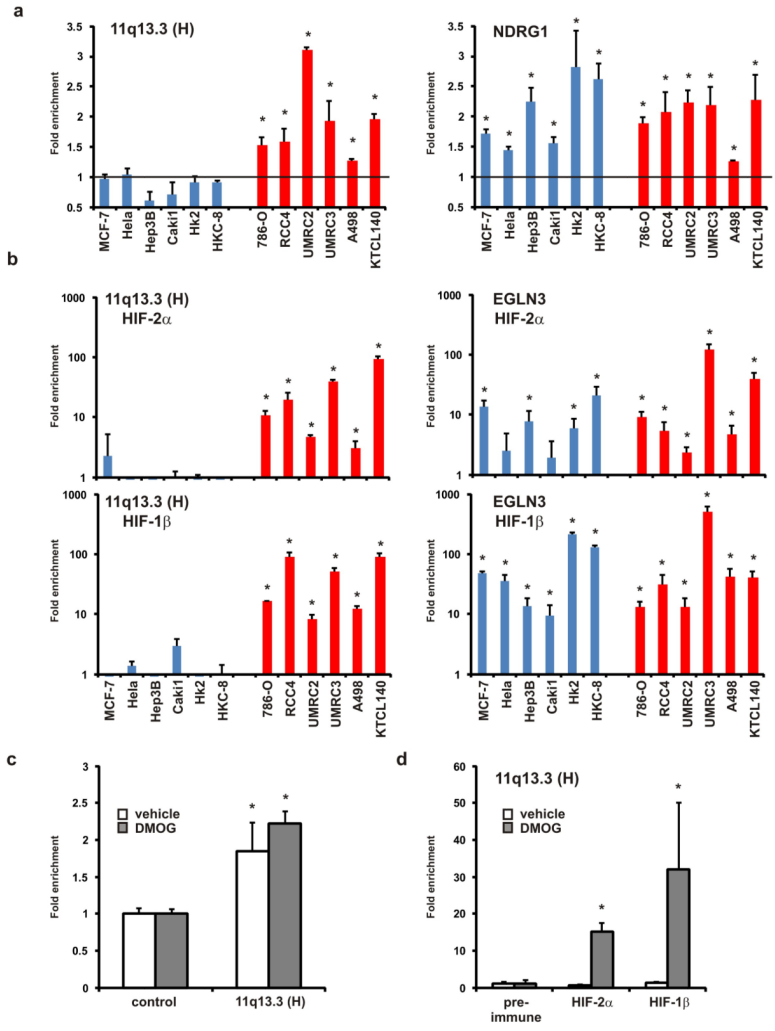

Figure 3. Cell-type specificity of the 11q13.3 enhancer

(a) FAIRE analysis; data is shown for a panel of six pVHL wild-type cell lines (blue) in which HIF was induced using HIF hydroxylase inhibitor dimethyl oxalylglycine (DMOG) and six pVHL-defective cell lines (red). qPCR products were normalized as described. Data in the left panel is the enrichment value for primers centered on the ChIP-seq signal (H); for comparison signals at the ubiquitous HIF-binding enhancer (*NDRG1)* are also given (right panel). **(b)** ChIP-qPCR results from the same panel of pVHL wild-type and pVHL-defective cell lines for HIF-2α (upper) and HIF-1β binding (lower) at 11q13.3 (H) (left panel); for comparison signals at the *EGLN3* locus are shown (right panels) **(c)** FAIRE analysis in 786-O cells re-expressing wild type pVHL (786-0/VHL cells). Data is the enrichment value for primers centered on the ChIP-seq signal (H) normalized to the control (non-enhancer) site; cells treated with or without DMOG to induce HIF **(d)** ChIP-qPCR analysis for HIF-2α and HIF-1β at the 11q13.3 H peak in 786-0/VHL cells treated with or without DMOG. Data is mean ± SD (n=3); *p<0.05 relative to pre-immune (ChIP) or to a control site (FAIRE).

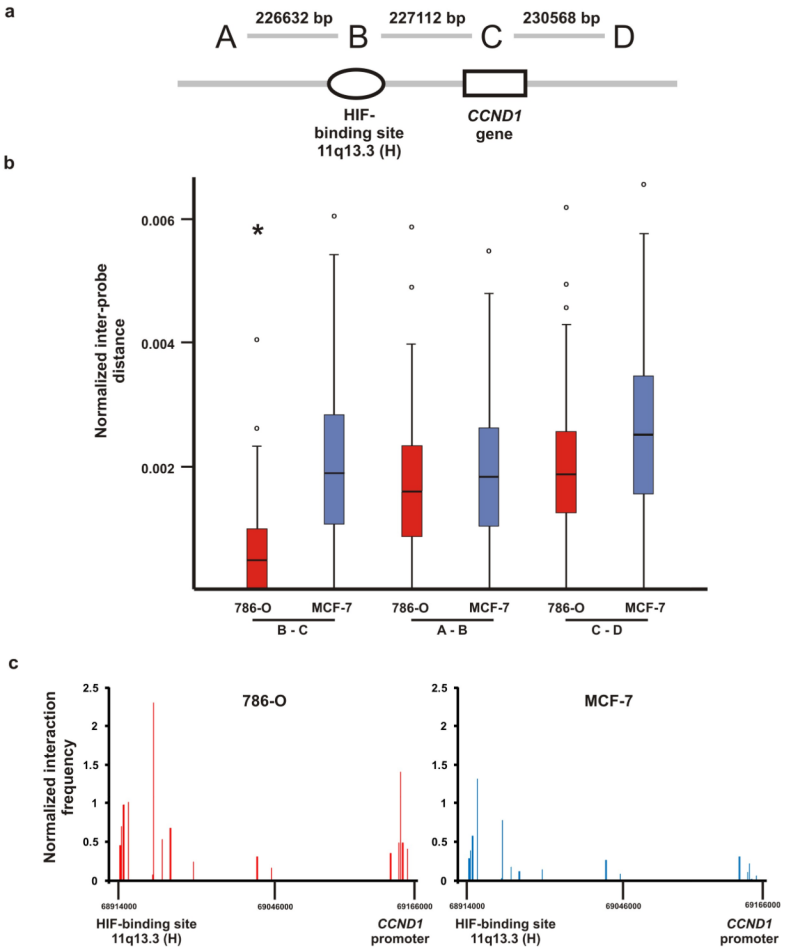

Figure 4. Physical association of the remote HIF-binding site with the *CCND1* promoter

(a) Location and distance between midpoints of fosmid probes used for 3-dimensional (3D) fluorescent *in situ* hybridization (FISH). **(b)** Box-and-whisker plots showing median, inter-quartile range and full range of visualized inter-probe distances for each pair of probes, normalized to nuclear volume. Kruskal-Wallis 1-way ANOVA was significant (P<0.001). Mann-Whitney U-test showed that probes at the HIF-binding site and the *CCND1* gene were significantly (*, p<0.001) more closely associated (in 786-O, but not MCF-7 cells) than were other probe pairs. **(c)** Chromatin conformation capture (3C) assays using the remote enhancer site as the anchor. Bars show qPCR analysis of the re-ligation frequency following restriction enzyme digestion, for cellular DNA, normalized to that of the BAC clones spanning the region of interest. Sites at the 11q13.3 HIF-binding locus preferentially ligated with fragments at the *CCND1* promoter in 786-O cells, but not in MCF-7 cells indicated a cell-type specific physical interaction.

Europe PMC Funders Author Manuscripts

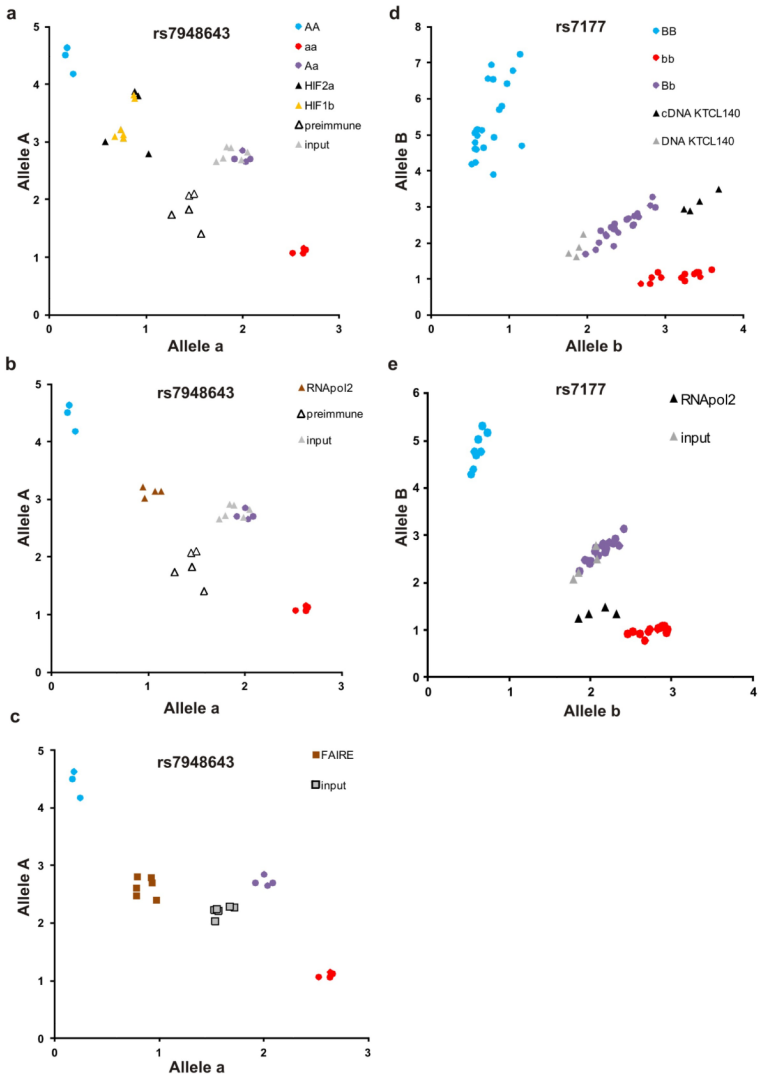

Figure 5. The minor (RCC-protective) allele at 11q13.3 disrupts HIF-binding and enhancer activity

(a) Genotype-specific PCR assays at the rs7948643 SNP, performed on immunoprecipitated chromatin from KTCL140 cells. The x-axis shows the intensity of the PCR signal for the minor (protective, a) and the y-axis shows intensity for the major (predisposing, A) allele. Control DNA from individuals homozygous (AA, aa) or heterozygous (Aa) for each allele was included for comparison in every assay. Input material and chromatin immunoprecipitated with pre-immune serum (control) showed an allelic ratio comparable to heterozygous DNA. Preferential recovery of allele A by HIF-2α and HIF-1β ChIP (yellow and black) demonstrates preferential binding of both subunits to this allele. **(b)** Genotype specific PCR assays at the rs7948643 SNP, performed on DNA immunoprecipitated from KTCL140 cells using an antibody directed against RNApol2 shows greater interaction of allele A with RNApol2. **(c)** Genotype specific PCR assays at the rs7948643 SNP, performed on KTCL140 DNA prepared by FAIRE. Preferential recovery of allele A indicates greater DNA accessibility. **(d and e)** Genotype specific PCR assay for rs7177, which lies in the 3′UTR of the *CCND1* gene using **(d)** cDNA from KTCL140 cells or **(e)** immunoprecipitated DNA using an antibody against RNApol2 show allele specific expression of *cyclin D1*. Genomic DNA from KTCL140 or control DNA from individuals

homozygous (BB, bb) or heterozygous (Bb) for each allele was included for comparison. Each symbol represents an individual PCR assay.

Europe PMC Funders Author Manuscripts